

SATELLITE MEASUREMENTS OF TRACE GASES USING BLIND SOURCE SEPARATION

Pia Addabbo, Maurizio di Bisceglie

Università degli Studi del Sannio
Piazza Roma 21, I-82100, Benevento, Italy

1. INTRODUCTION

Differential optical absorption spectroscopy (DOAS) [1] is a widely adopted technique for producing global estimates of trace gases and aerosols concentration from satellite observations. With this technique, several atmospheric components (e.g. O_3 , BrO , NO_2 , SO_2) as well as aerosol concentrations can be detected using the selective absorption structures in the UV and Visible portion of the spectrum. Essentially, DOAS can be used when some deep and clear absorption bands are induced by the molecular structure of the gas; an absorber that attenuates radiation, but has no clear molecular spectral structure in the sensed range of wavelength, is not suitable for measurement by DOAS.

Absorption spectroscopy is routinely used for *in situ* measurements of the ozone concentration in the atmosphere in a way which is very similar to that used in the laboratory. For low concentrations of the component or for moderate absorption rates, longer paths are necessary to obtain measurements with the required accuracy. Earlier instruments such as the Solar Backscatter UV (SBUV) measured the ozone column density by taking the ratios of a few wavelength pairs [2]. With the launch of the Global Ozone Monitoring Experiment (GOME) on the ESA satellite ERS-2 in 1995 [3], DOAS principles have been applied to satellite instruments with great success. Since GOME, retrievals have been produced for the SCanning Imaging Absorption spectroMeter for Atmospheric CHartography (SCIAMACHY) [4] on the ESA ENVironmental SATellite (ENVISAT), the Ozone Monitoring Instrument (OMI) on the NASA Earth Observing Satellite Aura (EOS-Aura) [5], and others instruments, using the DOAS technique.

OMI is the first of a new generation of spaceborne spectrometers that combine a high spatial resolution ($13 \times 24 \text{ km}^2$ at nadir) with daily global coverage. Total ozone from OMI data is currently obtained using the DOAS technique. Two other similar algorithms are also currently adopted for producing accurate measurements of SO_2 from OMI data: the Band Residual Difference (BRD) algorithm [6] and the Linear Fit (LF) algorithm [7]. The BRD is based on the evaluation of differential residuals due to the trace gas at several wavelength pairs; spectral bands are selected where large absorption peaks are displayed to improve the algorithm accu-

racy and discrimination from other gases [8]. The linear fit algorithm is based on fitting a linearized radiative transfer model plus a low-order polynomial to the logarithm of the reflectance spectrum. The methods are physically grounded and, at the current stage, are able to measure gas concentrations with a good level of accuracy [6,7].

We propose here a new method based on Blind Source Separation (BSS) of waveforms through [9]. Applications of BSS can be found in many different areas such as audio processing, biomedical signal processing, image processing, telecommunications, and econometrics.

In this work, we have considered separation of SO_2 contribution from OMI reflectance spectra. Major contributions to sulphur dioxide in the atmosphere come from both anthropogenic activities and natural phenomena, which include burning of fossil fuels in power plants, metal smelting, and volcanic emissions. Volcanic eruptions emit gases (H_2O , CO_2 , SO_2 , ...), ash particles and hydrometeors into the atmosphere, occasionally reaching heights of 20 km or more, to reside in the stratospheric overworld where they affect the radiative balance of the atmosphere and the Earth's climate.

2. OBSERVATION MODEL

The basis of spectroscopic measurements is Lambert-Beer's law. This law is a physical relationship that relates the absorption of the electromagnetic radiation to the properties of the surrounding medium. The law can be expressed as

$$I_1(\lambda) = I_0(\lambda) e^{-nl\sigma(\lambda)}, \quad (1)$$

where $I_1(\lambda)$ is the transmitted intensity of the radiation, $I_0(\lambda)$ the incident radiation, n the concentration of the medium [mol/cm^3], l the path length [cm], and $\sigma(\lambda)$ the absorption cross-section [cm^2/mol]. By expanding Lambert-Beer's law, one can consider the absorption of various trace gases with concentrations n_i and absorption cross-sections $\sigma_i(\lambda)$, that is

$$I_1(\lambda) = I_0(\lambda) e^{-l \sum_i n_i \sigma_i(\lambda)}. \quad (2)$$

The absorption cross-sections vary with temperature because the rotational and vibrational state distribution in the electronic ground state changes with temperature. Generally the

differential cross-sections increase with decreasing temperature. The SCIAMACHY pre-flight model [8] temperature-dependent absorption cross-sections of sulphur dioxide, obtained from 239 to 395 nm at five temperatures between 203 and 293 K, are plotted in Fig. 1.

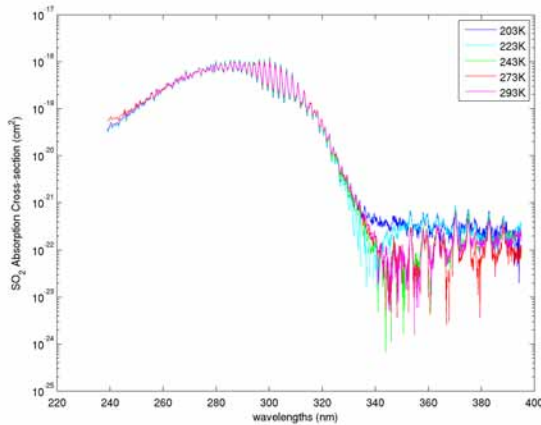


Fig. 1. SCIAMACHY temperature-dependent SO₂ absorption cross sections.

In any application of absorption spectroscopy, the quality of the reference cross-sections used, including their temperature dependence and resolution, is crucial for the accuracy of the results [10]. The basic principles of absorption spectroscopy apply for satellite measurements of scattered sunlight as like as measurements in the laboratory, but there are a number of complications that need to be accounted. First of all, the atmosphere is a mixture of different gases at varying concentrations. In addition, scattering by air molecules, aerosols and clouds as well as absorption from the ground, often dominate the extinction of sunlight. To separate these effects, measurements are taken at many different wavelengths simultaneously; individual absorbers can be identified and separated through their characteristic variation of absorption with wavelength. UV/VIS spectrometers, like OMI, detect the solar irradiance scattered and absorbed by the constituents of the atmosphere. For retrieving atmospheric trace gases in the UV/VIS wavelength range, it is therefore essential to measure the Earth radiance and solar irradiance spectrum, the latter serving as reference for the radiance spectrum. By normalizing the radiance spectrum by the solar irradiance spectrum, the reflectance spectrum is obtained, which is used as the primary spectrum for the retrieval of the atmospheric trace gases. It is interesting to note that the normalization has also the side effect of mitigating some instrument characteristics or degradation effects. The reflectance is defined as

$$R(\lambda) = \frac{\pi I(\lambda)}{\mu_0 E(\lambda)}, \quad (3)$$

where $I(\lambda)$ is the Earth radiance, $E(\lambda)$ the solar irradiance,

μ_0 the cosine of the solar zenith angle and λ the wavelength.

3. THE BLIND SEPARATION OF WAVEFORMS

The trace gas retrieval with blind source separation, involves three main steps:

1. Evaluation of reflectances.
2. Blind source separation.
3. Evaluation of trace gas concentration.

In this Section we illustrate the main issues related to these points with a specific reference to the Ozone Monitoring Instrument (OMI Level1b product).

3.1. Evaluation of reflectances

The reflectance, as defined in (3), is evaluated by interpolation of the OMI radiances and irradiances in the (270-330 nm) wavelength range. Interpolation is necessary for the doppler shift occurring between radiance and irradiance spectra. In the (270-330 nm) spectral range, several absorption features of the sulphur dioxide can be observed (see Fig. 1), although it is known that some interaction with the O₃ spectrum may cause errors in the estimation. OMI interpolated radiances and irradiances are shown in Figure 2.

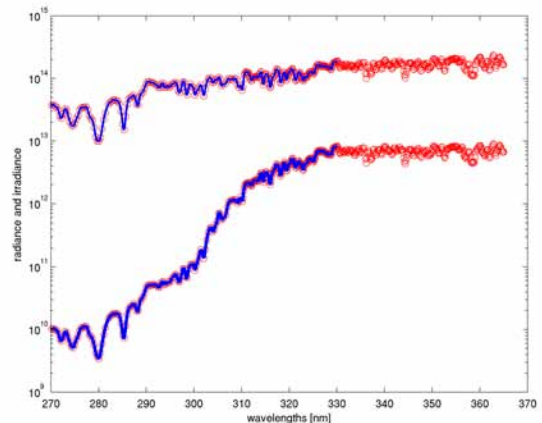


Fig. 2. OMI Interpolated Radiance and Irradiance spectra.

The negative logarithm of the reflectance is considered to take advantage of the linear dependence from the absorption cross sections and concentrations. According to the Beer-Lambert law, eq. (3) can be rewritten as [11]:

$$-\log(R(\lambda)) = -\log\left(\frac{\pi I(\lambda)}{\mu_0 E(\lambda)}\right) = l \sum_i n_i \sigma_i(\lambda) + const. \quad (4)$$

We use this quantity in our algorithm because the negative logarithm of reflectance is the superposition of weighted absorption cross-sections. Figure 3 shows an example of negative logarithm of OMI calculated reflectance spectrum.

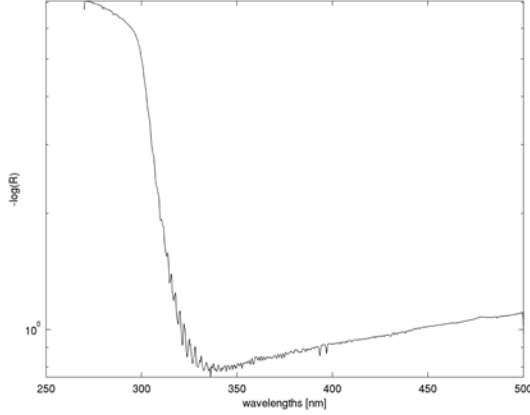


Fig. 3. Negative logarithm of OMI reflectance spectrum.

3.2. Blind Source Separation

We assume that the overall absorption from the atmosphere is due to statistically independent contributions; this is the main constraint to approach separation of the single reflectance spectra using Blind Source Separation. From m Instantaneous Field Of Views (IFOV) m spectra $[x_1(\lambda), x_2(\lambda), \dots, x_m(\lambda)]$, with λ the wavelength, are observed. They represent the linear combination (or mixing) of n unknown components $[s_1(\lambda), s_2(\lambda), \dots, s_n(\lambda)]$, with $n \leq m$, that are assumed to be mutually statistically independent. This assumption is physically grounded when statistical spectral dependencies due to chemical and physical gas interactions can be neglected. We let \mathbf{x} the vector of observations and \mathbf{s} the vector of independent components so we may write, using matrix notation, $\mathbf{x} = \mathbf{A}\mathbf{s}$. Here, \mathbf{A} is the unknown $m \times n$ mixing matrix. If we invert this equation, we obtain $\mathbf{s} = \mathbf{A}^{-1}\mathbf{x}$, so, the basic problem is to estimate \mathbf{A}^{-1} . In the absence of additional information about the single waveforms, the standard ICA works by maximizing the statistical independence of the components of \mathbf{s} . This task is usually carried out by ad-hoc algorithms, such as RADICAL (Robust Accurate Direct ICA algorithm) or Fast-ICA. This is, however, a simplified situation since we are not really concerned with a standard signal separation problem where the number of mixed sources is exactly known. In a trace gas estimation problem, in fact, the presence of all sources in any IFOV cannot be *a priori* assumed resulting in an ill-posed problem.

On the contrary, a nonzero trace gas concentration can be present only in some fields of view. This poses, in general, an additional problem embedded in the estimation procedure.

To overcome this difficulty, the problem can be restated as follows. For simplicity consider the case of a single trace gas to be separated; thus one observation is the mixture of a background waveform $s_1(\lambda)$ and a trace gas contribution $s_2(\lambda)$ that can be actually present or not. A second observation can be defined as a contamination of the former with a known SO_2 cross section waveform. Thus we may write

$$\begin{aligned} x_1(\lambda) &= a_{11}s_1(\lambda) + a_{12}\sigma_{SO_2}(\lambda), \\ x_2(\lambda) &= a_{21}s_1(\lambda) + a_{22}\sigma_{SO_2}(\lambda) + c_0\sigma_{SO_2}(\lambda), \end{aligned} \quad (5)$$

with c_0 the contamination factor and a_{12} possibly zero.

The procedure, applied to each IFOV of an OMI ascending or descending orbit, is summarized hereafter

1. two observations are defined as follows:

- the reflectance spectrum $x_1(\lambda)$ in a range of wavelengths (λ_1, λ_2) ;
- the contaminated spectrum $x_2(\lambda)$ in the same range of wavelengths, generated by injecting a light SO_2 component in the reflectance spectrum;

2. the mixing matrix is estimated by maximizing independence between spectra.

3. the spectral waveforms $[s_1(\lambda), s_2(\lambda)]$ are retrieved through matrix inversion.

The Robust and Accurate Direct ICA algorithm (RADICAL), based on maximization of the Mutual Information, is used for separating the SO_2 component of each OMI IFOV. The two observations, for each field of view, are

$$\begin{aligned} x_1(\lambda) &= -\log(R(\lambda)), \\ x_2(\lambda) &= -\log(R(\lambda)) + c_0\sigma_{SO_2}(\lambda), \end{aligned} \quad (6)$$

where $R(\lambda)$ is the reflectance, $\sigma_{SO_2}(\lambda)$ is the SO_2 absorption cross-section, and c_0 is the contamination factor. For the case at hand a reasonable value for c_0 is $2.69 \cdot 10^{16}$ [mol/cm²], corresponding to the concentration of 1 DU. Applying RADICAL algorithm to these two observations, we separate the SO_2 component from the overall atmospheric absorption. Therefore one of the two extracted components will be the SO_2 absorption cross section.

3.3. Evaluation of trace gas concentration

At this stage, an estimate of the SO_2 concentration is obtained by integrating the extracted SO_2 power spectrum as:

$$c_{SO_2} = \int |s_{SO_2}(\lambda)|^2 d\lambda, \quad (7)$$

where c_{SO_2} is the SO_2 concentration and s_{SO_2} is the SO_2 absorption cross section after blind source separation. This quantity is obviously the energy of the SO_2 signal. Energy

spectral densities for pixels having high (red line), medium (green line) and low (blue line) concentration are shown in Fig. 4.

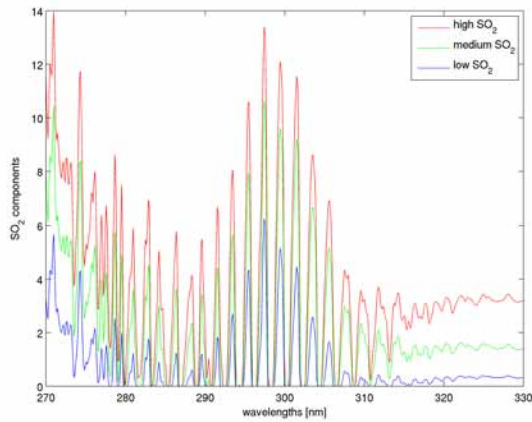


Fig. 4. SO_2 components with different concentrations.

4. RESULTS

In this section we present a case of large explosive volcanic eruption, the Kasatochi eruption on August 2008. Kasatochi Island is an active stratovolcano and one of the Aleutian Islands of southwestern Alaska, USA. On August 7, 2008, Kasatochi began erupting explosively with an ash plume maintaining an altitude of 10000 m and reaching 14000 m. Results obtained after processing the data acquired on August 9, 2008, using the Blind Source Separation algorithm are shown in Fig. 5.

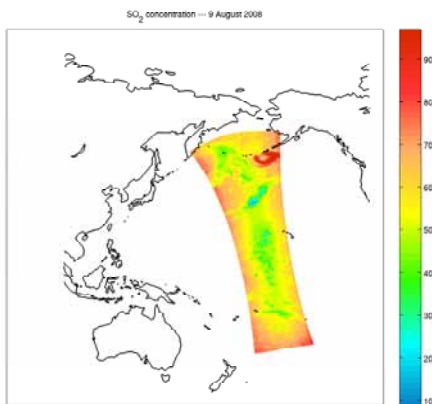


Fig. 5. SO_2 concentration from Kasatochi volcano eruption (August 9, 2008) using Blind Source Separation.

Figure 6 shows the corresponding image for the Planetary

Boundary Layer (PBL) SO_2 column processed using standard BRD algorithm from KNMI OMI team.

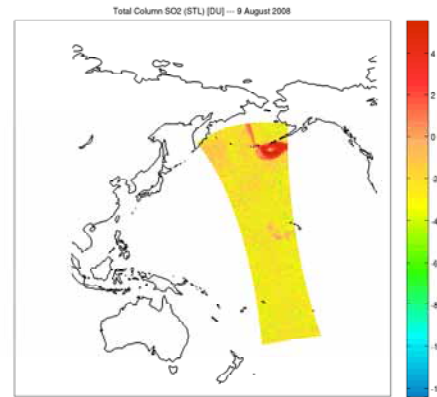


Fig. 6. SO_2 concentration from Kasatochi volcano eruption (August 9, 2008) using BRD algorithm.

Comparing the figures 5 and 6 we can see that the BSS algorithm is able to detect the SO_2 plume produced by the eruption of Kasatochi volcano. In Fig. 7 the OMI cloud fraction is represented to show the cloud features that can be also observed in Fig. 5 at the lowest levels.

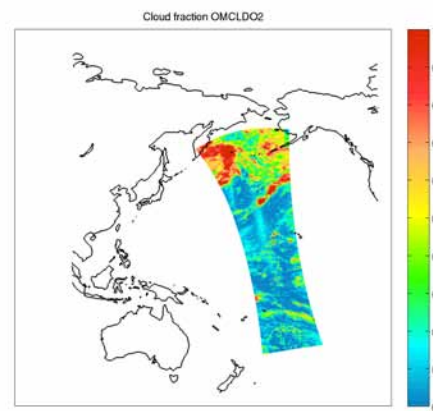


Fig. 7. OMI cloud fraction, (August 9, 2008)

In Fig. 8, a true color image from Aqua-MODIS on August 9, 2008, is shown to present a high resolution retrieval in the visible portion of the spectrum. High resolution cloud features are also clearly visible. Aqua orbit is 15 minutes before Aura orbit.

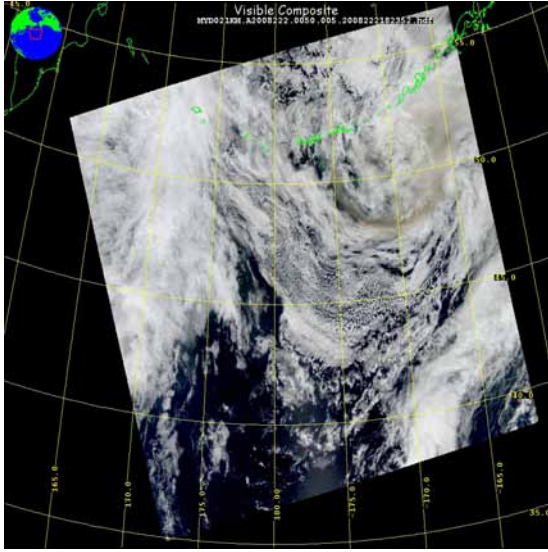


Fig. 8. Aqua Truecolor image, (August 9, 2008)

5. CONCLUSIONS AND FINAL COMMENTS

In this work, a new algorithm has been presented for estimation of trace gases concentration in the atmosphere. The main advantage is a more extensive use of the reflectance values retrieved in the useful UV band. Instead of using some differential observation taken from absorption lines, the main idea is to use the full waveform through a blind source separation algorithm, with the assumption that spectral waveform to be separated can be considered statistically independent. Results show that the algorithm is able to operate quite good but deeper investigation is required to assess performance and to validate results. More specifically, one important issue is to calibrate the retrieved values and show map concentrations in Dobson units or molecular densities. Validation also requires an extensive comparison between calibrated retrievals and results from canonical algorithms based on band residual difference and linear fit. Another issue regards the analysis of error induced by the blind separation procedure. The analysis requires a simulation stage where a known quantity of trace gas is placed in a layer at a given altitude. Preliminary results from MODTRAN software [12] simulations show that the procedure correctly separates the SO_2 contribution but some discrepancies between the retrieved (SO_2 -free) atmospheric reflectance and the expected one, still arise. Finally, contribution from clouds and other gases should be accounted for reducing the overall error.

References

[1] U. Platt and Jochen Stutz, *Differential Optical Absorption Spectroscopy*, Springer, 2008.

- [2] J.V. Dave and C.L. Mateer, "A preliminary study on the possibility of estimating total ozone from satellite measurements," *Journal of Atmospheric sciences*, vol. 24, 1967.
- [3] J.P. Burrows, M. Buchwitz, M. Eisinger, V. Rozanov, M. Weber, A. Richter, and A. Ladstaetter-Weissenmayer, "The global ozone monitoring experiment (GOME): Mission, instrument concept, and first scientific results," *Journal of Atmospheric sciences*, vol. 24, no. 2, 1999.
- [4] S. Noël, H. Bovensmann, J.P. Burrows, J. Frerick, K.V. Chance, and A.H.P. Goede, "Global atmospheric monitoring with SCIAMACHY," *Physics and Chemistry of the Earth*, vol. 24, no. 5, 1999.
- [5] P.F. Levelt, G.H.J. van den Oord, M.R. Dobber, A. Mälkki, H. Visser, J. de Vries, P. Stammes, J.O.V. Lundell, and H. Saari, "The ozone monitoring instrument," *IEEE Transactions on geoscience and remote sensing*, vol. 44, no. 5, May 2006.
- [6] N.A. Krotkov, S.A. Carn, A.J. Krueger, P.K. Bhartia, and K. Yang, "Band residual difference algorithm for retrieval of SO_2 from the Aura Ozone Monitoring Instrument (OMI)," *IEEE Transactions on geoscience and remote sensing*, vol. 44, no. 5, May 2006.
- [7] K. Yang, N.A. Krotkov, A.J. Krueger, S.A. Carn, P.K. Bhartia, and P.F. Levelt, "Retrieval of large volcanic SO_2 columns from the aura ozone monitoring instrument: Comparison and limitations," *Journal of Geophysical Research*, vol. 112, 2007.
- [8] K. Bogumil, J. Orphal, T. Homann, S. Voigt, P. Spietz, O.C. Fleischmann, A. Vogel, M. Hartmann, H. Kromminga, H. Bovensmann, J. Frerick, and J.P. Burrows, "Measurements of molecular absorption spectra with sciamachy pre-flight model: instrument characterization and reference data for atmospheric remote-sensing in the 230-2380 nm region," *Journal of Photochemistry and Photobiology*, 2003.
- [9] A. Hyvärinen and E. Oja, "Independent component analysis: Algorithms and applications," *Neural Networks*, 2000.
- [10] A. Richter, "Differential optical absorption spectroscopy as tool to measure pollution from space," *Spectroscopy Europe*, vol. 18, 2006.
- [11] *OMI Algorithm Theoretical Basis Document Volume IV*, August 2002, http://www.knmi.nl/omi/documents/data/OMI_ATBD_Volume_3_V2.pdf.
- [12] A. Berk, L.S. Bernstein, and D.C. Robertson, "Modtran: A moderate resolution model for lowtran 7," *Air Force Geophysics Laboratory Technical Report GL-TR-89-0122*, 1989.